Proceedings of Ninth World Conference on Earthquake Engineering
August 2-9, 1988, Tokyo-Kyoto, JAPAN (Vol.IV)

6-2-10

FRACTURE AND DEFORMATION CAPACITY OF A WELDED T-SHAPE JOINT UNDER DYNAMIC LOADING

Tadao NAKAGOMI[1] and Hiroaki TSUCHIHASHI[2]

[1]Department of Architecture and Building Engineering, Shinshu University, Wakasato, Nagano, Japan
[2]Kumagaigumi Co., Ltd., Shinjyukuku, Tokyo, Japan

SUMMARY

Influence of strain velocity to mechanical property and transient phenomenon from ductile to brittle fracture on connection hasn't been studied. So, we did an experiment for researching influences of strain velocity and temperature to fracture behaviours in order to propose the way of evaluating earthquakeproof designs. As results, transient temperatures under dynamic loading is higher than static ones, and maximum dynamic $\bar{J}$-value is also higher than static one. The phenomenon that deformation capacities decreased remarkably at below transient temperature on the T-shape specimen test is explained by using a relationship between transient temperature of K_{ic} and of K_{id}.

INTRODUCTION

It is predicted that structures subject to dynamic external force deform with high velocity displacement. Particularly, velocities of a relative stored displacement on large structures are expected to be more than 50 cm/sec or sometimes 100 cm/sec. It is considered that the averaged strain velocities at steel elements or beam-column connections in a steel structure must be about 0.1/sec (Ref. 1) when the structure subject to the dynamic external forces. These deformations at beam-column connections are especially important function in order to design a earthquakeproof steel structure. But most of previous researches have investigated only mechanical properties of the beam-column connections or steel elements based on statical experiments. Furthermore, the dependence on strain velocities to the mechanical property of steel materials has been indicated (Ref. 2) for a long time. But the influence of strain velocities to the mechanical property on some appropriate parts such as connections involving stress concentration or metallurgical discontinuity have not been investigated till now.

Also it is well-known that temperatures influence the mechanical property of a steel material. But the transient phenomenon from ductile fracture to brittle fracture or fracture behaviors itself have been studied scarcely even at the temperatures which structures are exposed (about -10°C - about +50 °C). Further, any experiment on the fracture behavior of steel elements (Ref. 3) has not been done under both of two conditions described above, changing temperatures and changing load velocities, at all.

Therefore, this paper deals with the mechanical test to investigate the influences of strain velocities and temperatures, and with the experiment using welded T-shape specimen of a welded connection in order to obtain some basic data

for evaluation of earthquakeproof design.

MATERIAL TEST

Method of Test The tensile test pieces were extracted from a steel plate (SM50A, 36) which was also applied to welded T-shape specimens. Configuration of the test piece was finished to be same shape as 14A test piece of Japan Industrial Standard as shown in Fig. 1. Table 1 shows loading velocities and test temperatures as test parameters, and it also shows labels of the test pieces. Chemical compositions of the steel plate and results of Charpy impact test are shown in Table 2, Table 3 respectively. A testing machine for fatigue test (Maximum load 35tf and maximum loading velocity 20cm/s) was used in the case of high loading velocities, and an almighty elaborate testing machine (Maximum load 10tf) was used for the statical test. When low temperature test was taken place, the temperature was measured by using a thermocouple put on the test piece, and the temperature was kept within +- 0.5°C from the desired temperature for more than 30 minutes. In regard to the high loading velocity test, the load was measured with load cell, displacement was measured with a optical displacement measuring device (gauge length 50mm) and strain was measured by putting wire strain gauges at middle of the test piece.

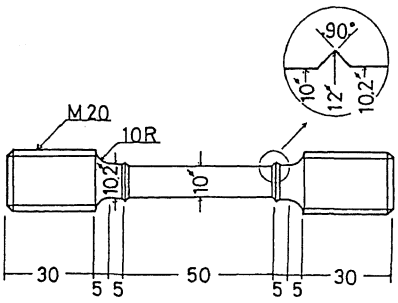

Fig. 1 Tensile Specimen of Material Test

Table 1 List of Tensile Specimen

Temperature \ Load Velocity	0.0017cm/s	※	0.1cm/s	※	1cm/s	※	10cm/s	※	100cm/s	※
Room temp	V1R	3	V2R	4	V3R	2	V4R	2	V5R	2
0°C	—	-	V2Z	1	—	-	V4Z	1	V5Z	1
-20°C	—	-	V2L	1	—	-	V4L	1	V5L	2

※Number of specimens

Table 3 Result of Shalpy Impact Test

SM50A 鋼36	Absorbed Energy (kgf·m)	Percent Brittle Fracture (%)	Transient Temperature (°C)
Rolling Direction	10.5	55.0	1.0
Right Angle to Rolling Direction	6.1	53.3	3.0
Thickness Direction	1.5	87.5	16.0

Absorbed energy and percent brittle fracture are value at 0°C.

Transient temperature is the temperature when percent brittle fracture is 50%.

Table 2 Chemical Composition of Material Test (%)

	C	Si	Mn	P	S	Cu	Ni	V	Cr
SM50A 鋼36	0.17	0.36	1.45	0.020	0.010	0.17	—	—	0.15

Result of Test Table 4 shows results obtained from t[illegible] test. These results are shown as average values in this Table. Syu [illegible] the Table are indicated as nominal stress and Est means percentage elo[illegible] Comparisons of each loading velocities at room temperature are shown [illegible] 2, and also comparisons of each temperatures (Load velocity 100cm/s) [illegible]sented in Fig. 3. It is considered from these figures that the effect [illegible]ncreasing load velocity is similar to the effect of rising the tempera[illegible]ld stress and ultimate stress become higher in proportion to increasi[illegible] velocity (or rising the temperature). Increasing ratios of upper yi[illegible] and ultimate stress subsequent to the increasing of loading velocity [illegible]n Fig. 4 and Fig. 5 respectively. Longitudinal axis of these figures [illegible]e values which are divided by the stress of statical loading at room te[illegible] so that these values are dimensionless quantities. Each curves [illegible] figures show approximation lines by using the least squares method rep[illegible] following:

$$Syu/Syu_o=1.378+0.125\log_{10}\dot{e}_e+0.010(\log_{10}\dot{e}_e)^2 \quad (1)$$

$$Su/Su_o=1.030+0.023\log_{10}\dot{e}_p+0.004(\log_{10}\dot{e}_p)^2 \quad (2)$$

Relationship between upper yield stress ratio and loading velocity, and also relationship between ultimate strength ratio and loading velocity are shown in Fig. 6 and Fig. 7 respectively. It must be obvious from these figures that increasing ratios at lower temperature are larger than higher one.

Table 4 Result of Tensile Test

	Syu (kgf/mm²)	Syl (kgf/mm²)	εst (%)	Su (kgf/mm²)	δf (%)	Φ (%)	Yu (Syu/Su)	Yl (Syl/Su)	ε̇e (1/s)	ε̇p (1/s)
V 5 R	49.6	44.1	2.57	59.9	31.9	72.9	0.828	0.735	2.9	1.1×10^{1}
V 4 R	43.0	40.4	2.02	58.0	30.0	70.8	0.741	0.697	1.1×10^{-1}	2.0
V 3 R	38.7	37.0	2.10	55.7	28.1	71.6	0.695	0.664	1.0×10^{-2}	1.8×10^{-1}
V 2 R	37.8	36.1	2.12	54.5	28.9	71.7	0.683	0.662	4.9×10^{-4}	1.9×10^{-2}
V 1 R	34.0	33.3	1.52	52.6	31.1	71.5	0.649	0.633	2.9×10^{-6}	1.6×10^{-2}
V 5 Z	52.7	46.3	1.49	62.0	30.6	71.4	0.851	0.748	2.6	1.1×10^{1}
V 4 Z	43.3	42.1	1.60	59.5	28.9	70.4	0.728	0.708	1.1×10^{-1}	1.9×10^{-1}
V 2 Z	39.5	38.3	1.44	57.4	29.3	71.1	0.688	0.668	1.2×10^{-3}	1.7×10^{-2}
V 5 L	57.5	43.3	2.52	63.0	32.7	71.9	0.914	0.688	3.1	1.3×10^{1}
V 4 L	49.2	44.5	2.62	61.3	25.9	67.9	0.802	0.720	1.3×10^{-1}	1.9
V 2 L	40.4	38.7	1.80	58.3	29.4	71.5	0.693	0.663	1.7×10^{-3}	1.8×10^{-2}

S_{yu}: Upper yield stress　δ_u: Uniform elongation
S_{yl}: Lower yield stress　δ_f: Strain at failure
S_u: Ultimate stress　ϕ: Reduction of section area
ε_{st}: Strain at the beginning of strain hardening
Y_u: Ratio of upper yield stress to ultimate stress
$\dot{\varepsilon}_p$: Strain velocity during plastic deformation

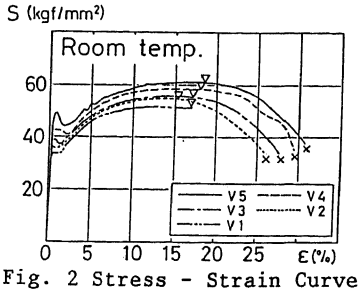

Fig. 2 Stress - Strain Curve

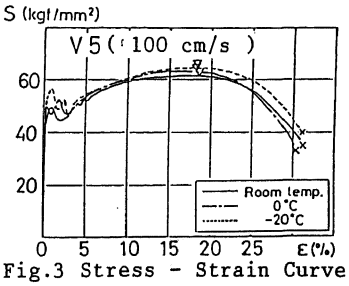

Fig.3 Stress - Strain Curve

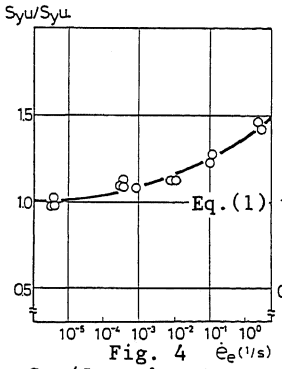

Fig. 4 $\dot{\varepsilon}_e$(1/s)
Syu/Syu₀-$\dot{\varepsilon}_e$relation
at room temperature

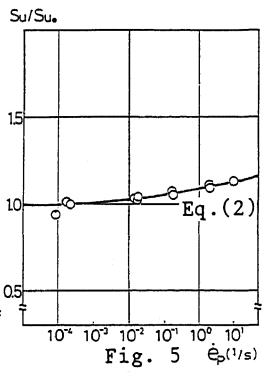

Fig. 5 $\dot{\varepsilon}_p$(1/s)
Su/Su₀-$\dot{\varepsilon}_p$relation
at room temperature

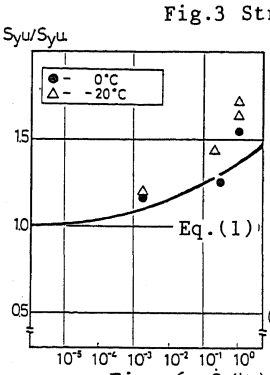

Fig. 6 $\dot{\varepsilon}_e$(1/s)
Syu/Syu₀-$\dot{\varepsilon}_e$relation

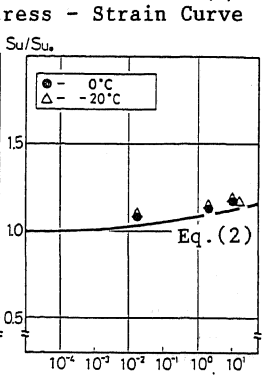

Fig. 7 $\dot{\varepsilon}_p$(1/s)
Su/Su₀-$\dot{\varepsilon}_p$relation

BEND TEST OF WELDED T-SHAPE JOINT

Specimen The specimens applied in this test were modeled as T-shape which is extracted from an actual beam-column connection as shown in Fig. 8. The configuration and it's scale is shown in Fig. 9. List of the specimens are shown in Table 5. Two different types of specimens were prepared for the test. Every specimens have a backing strip, but only one type of backing strips were welded by fillet welding as tack welding and the others were made without tack weldings. Three loading velocities (0.0025cm/sec, 0.25cm/sec and 25cm/sec) and also three different temperatures (-20°C, 0°C and room temperature) were selected as the test condition. The welding was done as the single bevel groove and it's angle was 35, and the root gap of the welding was 6mm. CO2semi-automatic gas shielded arc welding was done for the specimens with flat position. The detail of the welding conditions are shown in Table 6.

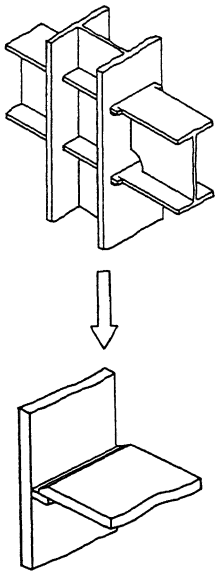

Fig. 8 The Way of Modelling the T-shape Specimen from Beam-Column Conjunction

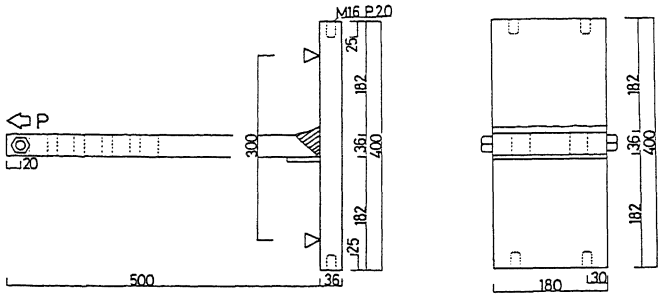

Fig. 9 Configulation and Size of T-shape Specimen

Table 5 List of T-shape Specimen

Temperature / Load Velocity	non tack welding						tack welding			
	Room temp. (R)	※	0°C (Z)	※	-20°C (L)	※	Room temp. (R)	※	-20°C (L)	※
0.0025cm/s (S)	SR-	3	SZ-	2	SL-	1	TSR-	1	TSL-	1
0.25cm/s (Q)	QR-	2	QZ-	1	QL-	1	—	-	—	-
25cm/s (D)	DR-	4	DZ-	1	DL-	1	TDR-	1	TDL-	1

※ Number of specimens

Table 6 Welding Condition

Welding Current (A)	Ark Voltage (V)	Welding Speed (cm/s)	Weld Wire (Φ)	Amount of CO2 Gas Flow (l/min)
310-380	39-42	20-30	1.4	30

Loading Method A dynamic servo fatigue testing machine (max. 75tf, 20cm/sec) was used for the loading in the test. The loading direction is altogether shown in Fig. 9. Statical loading was given until it reaches 1tf in every case, and then the required loading velocity was given to the specimens. When the test under low temperature was performed, the desired temperature was kept for more than 30 minutes by putting into a fluid that consist of Etyl alcohol and Dry Ice before the loading was given.

Method of Measurement Loading value was measured with a load cell, displacement was measured with differential transformer and strain was measured with wire strain gauges put around the welded zone. Obtained values from the test were recorded in a data recorder and then these data was converted with a A/D conversion device for using micro computer during dynamic loading.

Result and Consideration

Fracture Pattern All results of the test is shown in Table 7. Fracture forms can be roughly classified into 6 different types as shown in Fig. 10. The dotted lines in these figures indicate the regions where ductile fracture occurred, and solid lines indicate the regions of brittle fracture. The specimens of type 1 - type 3 were made without tack weldings of the backing strips and type 4 - type 6 were with tack welding. It is considered that fracture forms depend on the loading velocities, temperatures or whether tack welding was done or not. Particularly in case of the test under -20°C, every specimens were broken as type 1 and also all of these fractures surface were completely brittle one. A tendency that the region of ductile fracture become smaller as loading velocity become higher was recognized under the test of 0°C. In regard to the test at the room temperature, fracture started from the root of the single bevel groove or the end of welding reinforcement, and percent ductile fracture become larger in proportion to the loading velocity become higher in a ductile-brittle fracture surface. Cracks propagated from the end of the welding reinforcement on every specimens which were made with the tack welding.

Table 7 Result of T-shape Specimens Test

specimen	Py (tf)	δy (mm)	δu (mm)	δf (mm)	Pmax (tf)	Failure shape	Temperature (°C)	J (kgf/mm)	Length of Ductile Crack (mm)
SR-1	38.5	2.32	49.9	68.0	65.7	③	15.5	4231	6.0
SR-2	39.6	2.20	--	41.6	(68.3)	③	15.8	3399	1.5
SR-3	39.4	2.16	46.2	48.2	70.9	②	15.0	4155	5.0
QR-1	41.6	2.73	46.1	51.4	69.1	②	15.0	4104	8.0
QR-2	43.2	2.49	47.4	58.6	71.7	②	15.0	4486	7.0
DR-1	49.2	3.11	--	--	--	-	16.3	--	--
DR-2	50.1	3.47	47.9	>86	74.7	-	14.2	5098	--
DR-3	50.2	3.69	49.7	93.9	72.6	②	14.4	4901	12.0
DR-4	49.2	3.11	47.2	>90	74.2	③	14.7	4644	10.0
SZ-1	37.3	2.16	39.5	58.2	66.0	②	0±2	3309	5.5
SZ-2	38.2	2.15	--	44.9	(69.7)	②	0±2	3988	1.0
QZ-1	41.8	2.25	--	42.0	(69.9)	②	0±2	3752	2.0
DZ-1	50.7	3.23	--	21.4	(63.7)	①	0±2	1697	1.0
SL-1	40.7	2.65	--	12.9	(54.8)	①	-20±2	850	0.0
QL-1	44.0	2.98	--	9.2	(51.7)	①	-20±2	565	0.0
DL-1	--	--	--	2.3	(48.8)	①	-20±2	54	0.0
TSR-1	39.6	2.15	--	16.5	(57.2)	⑥	17.0	1153	3.5
TDR-1	49.6	2.95	48.1	>90	(47.5)	⑥	13.1	4811	15.0
TSL-1	40.6	2.86	--	7.2	47.5	⑤	-20±2	368	2.5
TDL-1	--	--	--	2.3	(53.1)	④	-20±2	122	0.0

Py: Yield load Pmax: Maximum load δU: Displacement at failure
δU: Displacement at maximum load δy: Displacement at yield load

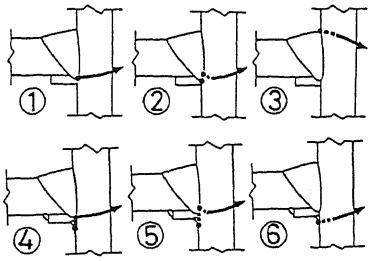

Fig. 10 Six Patterns of Failure Shape

$$\overline{J} = \frac{1}{B \cdot t} \int_0^{\delta(Pmax)} P d\delta$$

B: Width
t: Thickness

Load - Displacement Relationship Fig. 11 shows load - displacement curves obtained from the test at room temperature. It is recognized that both of the yield strength and the ultimate strength shift to higher values as loading velocity become higher. But there is not consistent tendency or certain order about the displacement after fracture in this temperature. Fig. 12 also shows load - displacement curves obtained from the test at 0°C. Both of the yield strength and ultimate strength shift to higher values and the displacement after fracture shift to smaller as loading velocity become higher in this figure. The same tendencies (as the curves at 0°C) are recognized in Fig. 13 which shows the same curves under -20°C. Further, Fig. 14 shows a load - deformation curves for comparison between the specimens with the tack welding and the ones without it (statical loading, room temperature). It is clearly recognized from this figure that the specimens with the tack welding broke at smaller deformation than the specimens without it. This tendency could be observed even in any temperatures or loading velocities.

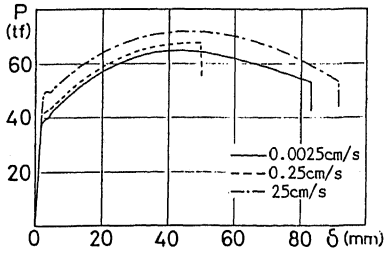

Fig. 11 Load - Deformation Curve (Room Temperature)

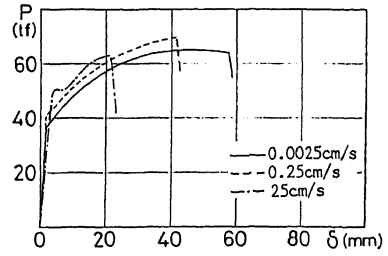

Fig. 12 Load - Deformation Curve (0°C)

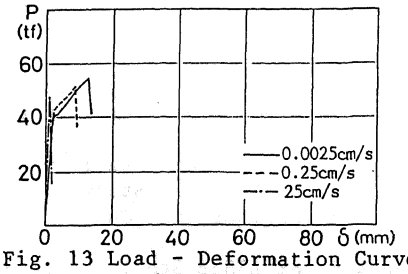

Fig. 13 Load - Deformation Curve (-20°C)

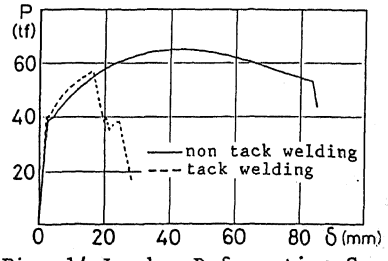

Fig. 14 Load - Deformation Curve for Comparison

Effect of Loading Velocity and Temperature Relationship between the displacement after fracture and the loading velocity during elastic region is shown in Fig. 15. The displacement after fracture become larger according to the loading velocity shift to higher value at -20°C and 0°C. Contrary to this, opposite tendency is observed at room temperature as shown in the figure. A comparison between Kıc (statical fracture toughness) and Kıd (dynamic fracture toughness) of A553B steel is shown in Fig. 16. *These values of Kıc or Kıd were quoted from the report* introduced as Ref. 4. It is shown in this figure that the transition temperature of Kıd is higher than the one of Kıc. Also Kıc is larger than Kıd in the region below the transition temperature of Kid, but the former become smaller than the latter in the region above the temperature. Fig. 17 shows comparisons of three different J-values (three different loading velocities) obtained from the test. Three curves in the figure represent a typical pattern of the transition curve. It is considered from this figure that the transition temperature shifts to high when loading velocity becomes high in the same manner as Fig. 16.

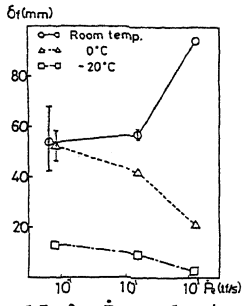

Fig. 15 δf-Ṗe relation

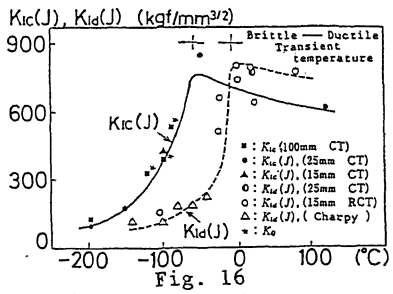

Fig. 16 Comparison of Kıc with Kıd (Ref. 4)

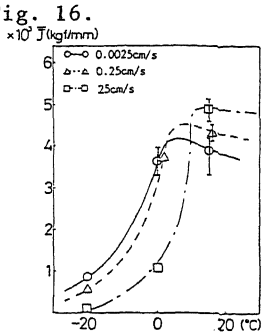

Fig. 17 Comparison of Three Different J̄-values

CONCLUSION

(1) Both of yield strength and ultimate strength shift to large as rising the temperature or increasing the loading velocity in case of the material test. But ultimate strength or fracture toughness decrease remarkably according to increase the loading velocity at below the transition temperature in case of T-shape specimen which is influenced considerably by strain concentration.

(2) The phenomena that deformation capacity changes according to the loading velocity or test temperature could be explained by using the relationship between Kıc and Kıd.

REFERENCES

1. H. Aoki, B. Kato et al., "Influences of Test Temperature and Load Velocity on Ultimate Strength and Deformation of Notched Steel Elements," Transactions of The Architectural Institute of Japan, 11-19, Dec., (1982).
2. K. Kawada, "Impactproof of Rigid and New Developed Measuring Method for It," Proceedings of The Second Material Impact Problems Symposium, Institute of Material of Japan, 25-32, Jan., (1987).
3. M. Fujimoto, T. Nakagomi et al., "Study on Fracture of Steel Construction Connection by Non Linear Fracture Mechanics (Part 2 Study on Fracture Properties of Tee Welded Joints)," Transactions of The Architectural Institute of Japan, 63-72, Jan., (1976).
4. T. Iwadate et al., "Experimental Study on Kıd of A553B Steel," Summaries of Technical Papers of Annual Meeting JSME, 790-12, 232- , (1979).